

The (dynamically-driven) diurnal cycle in the SEP

* Does it exist?

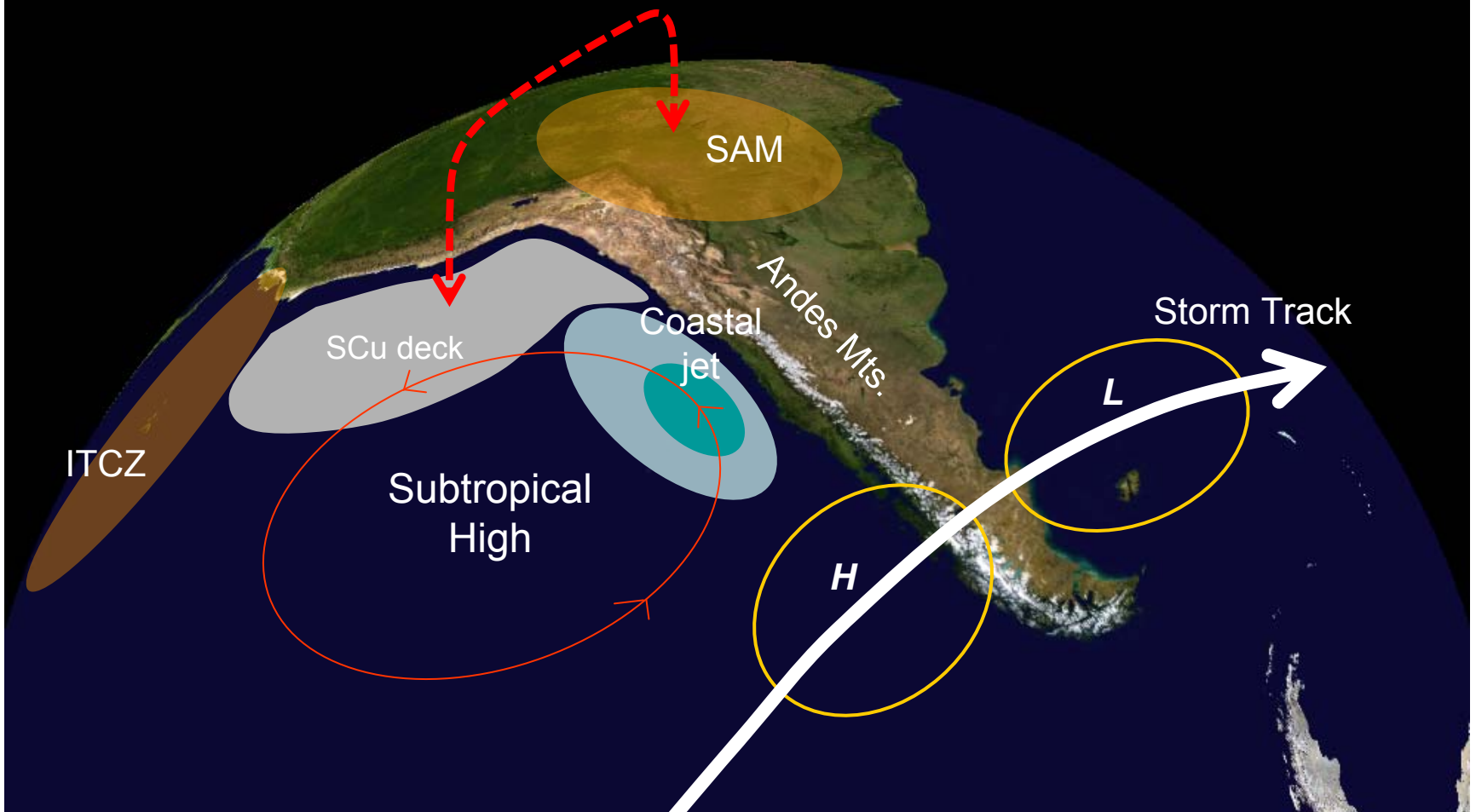
* Does it impact clouds?

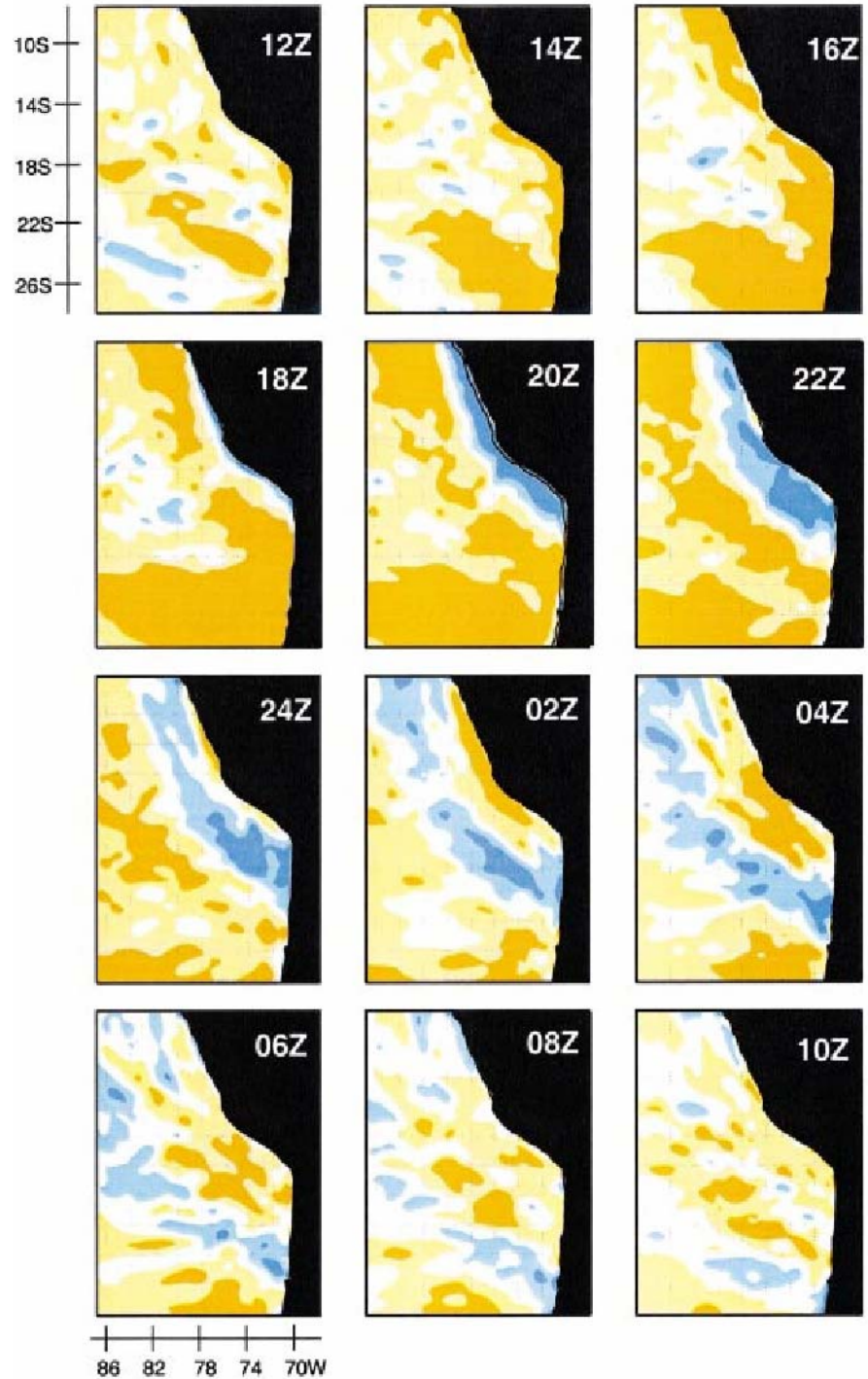
René D. Garreaud, Ricardo Muñoz,
Dave Rahn and José Rutllant

*Department of Geophysics
Universidad de Chile*

Key atmospheric features over the SEP

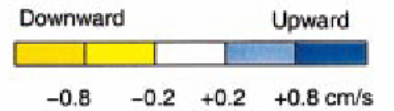
VAMOS: Dynamical link between South American Monsoon and SEP, first suggested by Gandau and Silva-Dias (1998)





**MM5 results
SON simulation**

◀ **Mean diurnal
cycle of vertical
velocity at 800 hPa**



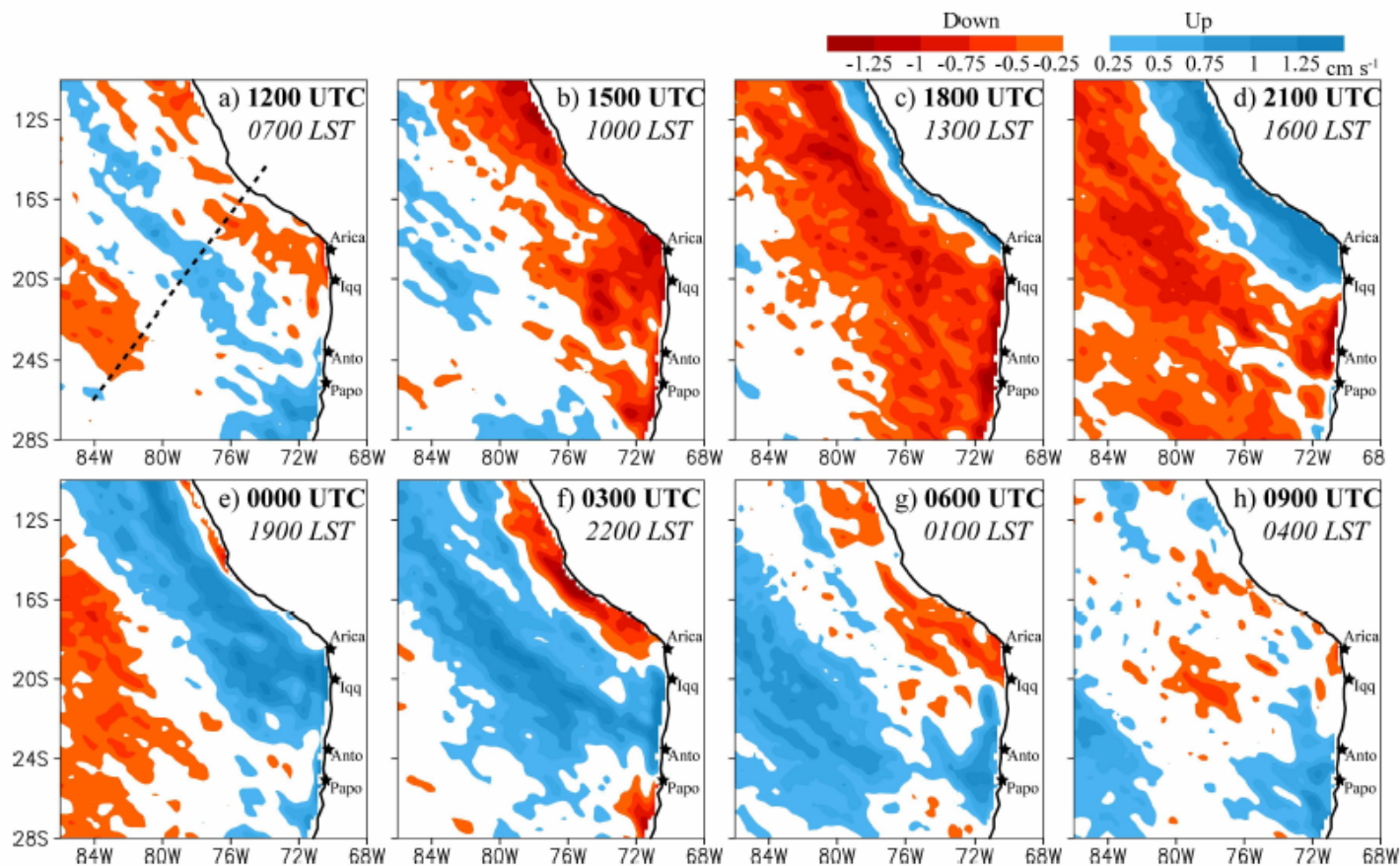
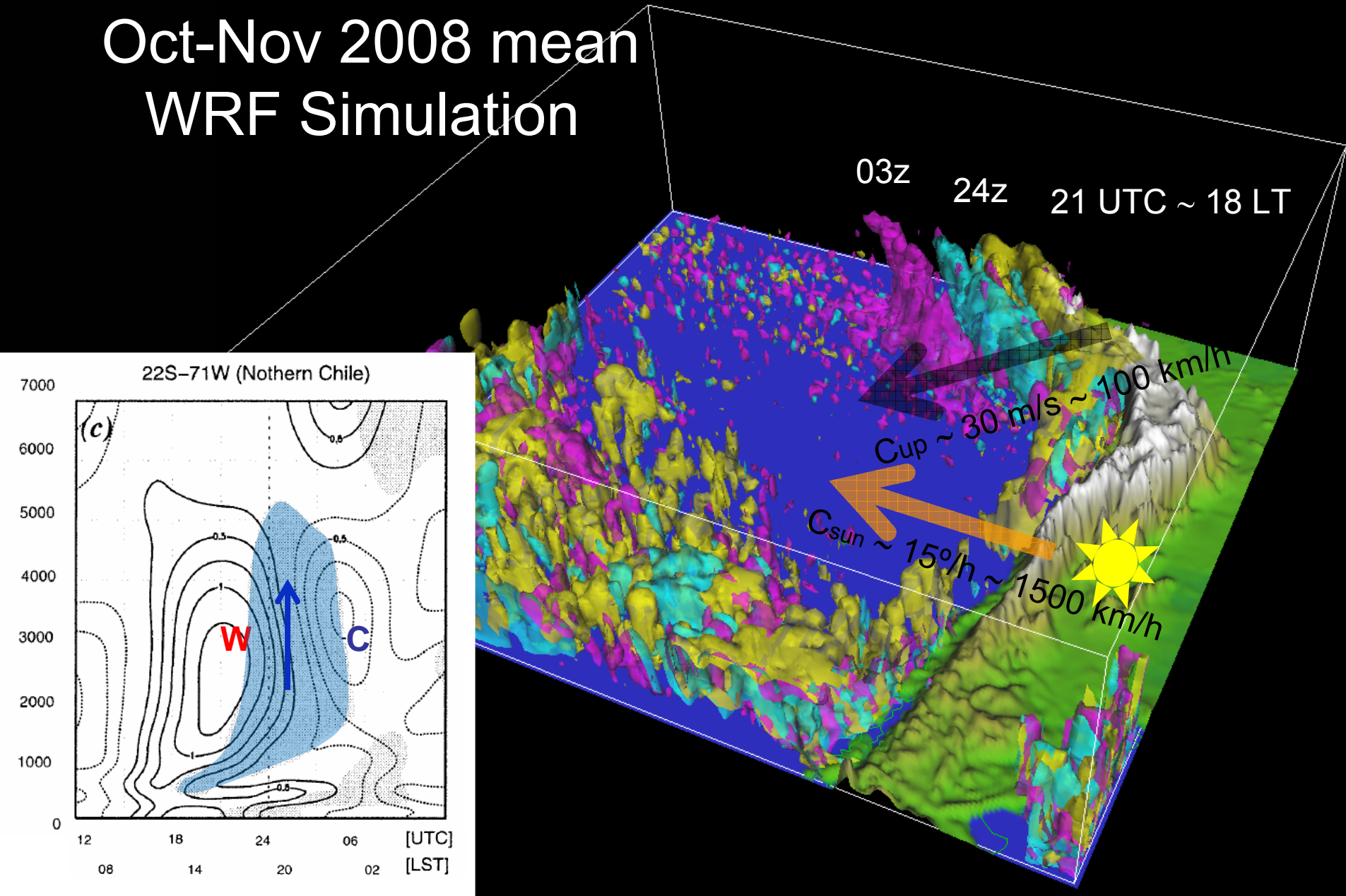
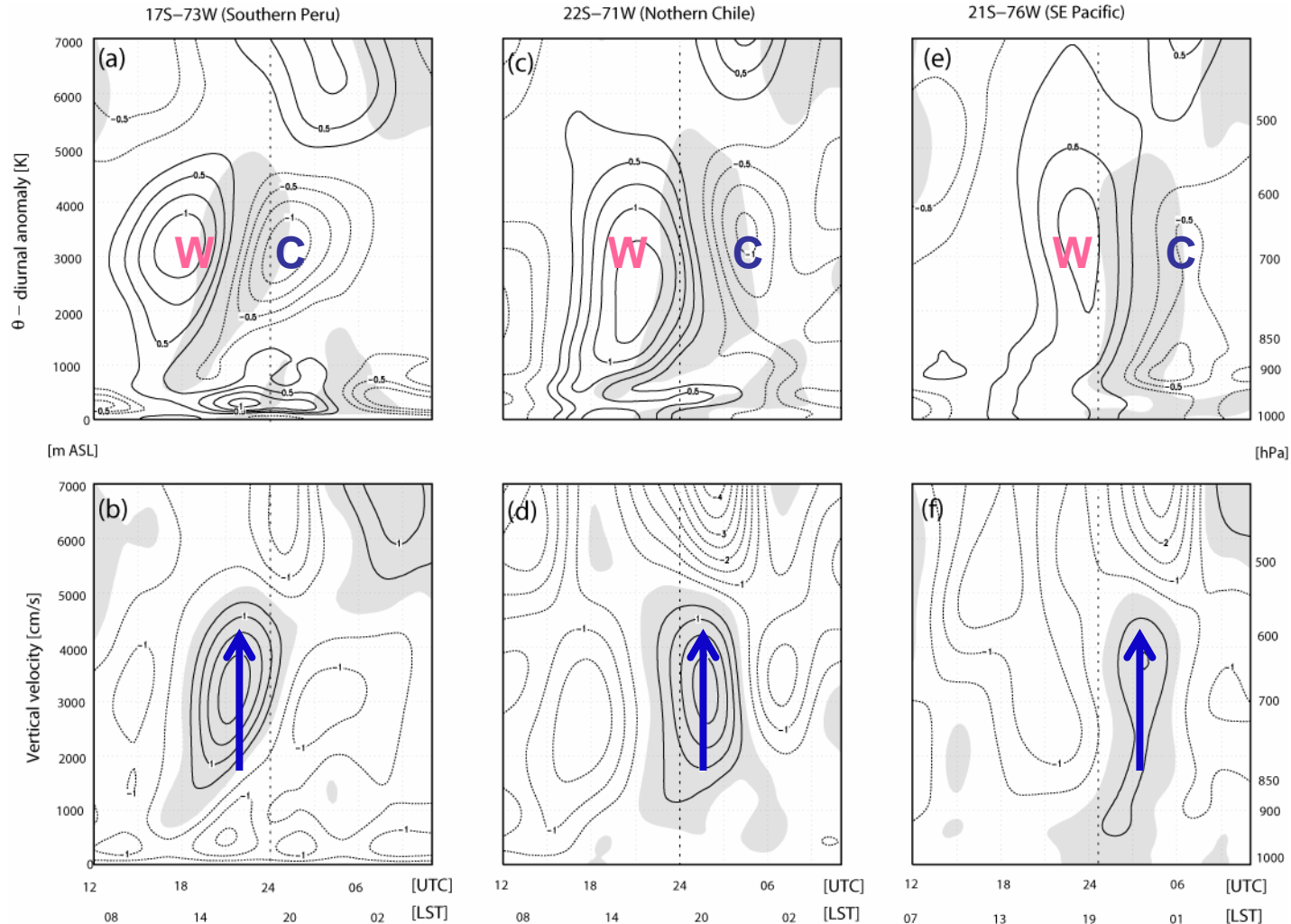


Fig. 9. WRF-simulated 2-month mean diurnal vertical velocity anomalies (cm s^{-1}) at 2.5 km every 3 hours. Red (blue) indicates downward (upward) motion. Dashed line in (a) depicts location of subsequent cross section. Also shown is the location of the coastal sounding stations during VOCALS-REX.

Isosurface $w < -0.1$ mm/s Oct-Nov 2008 mean WRF Simulation



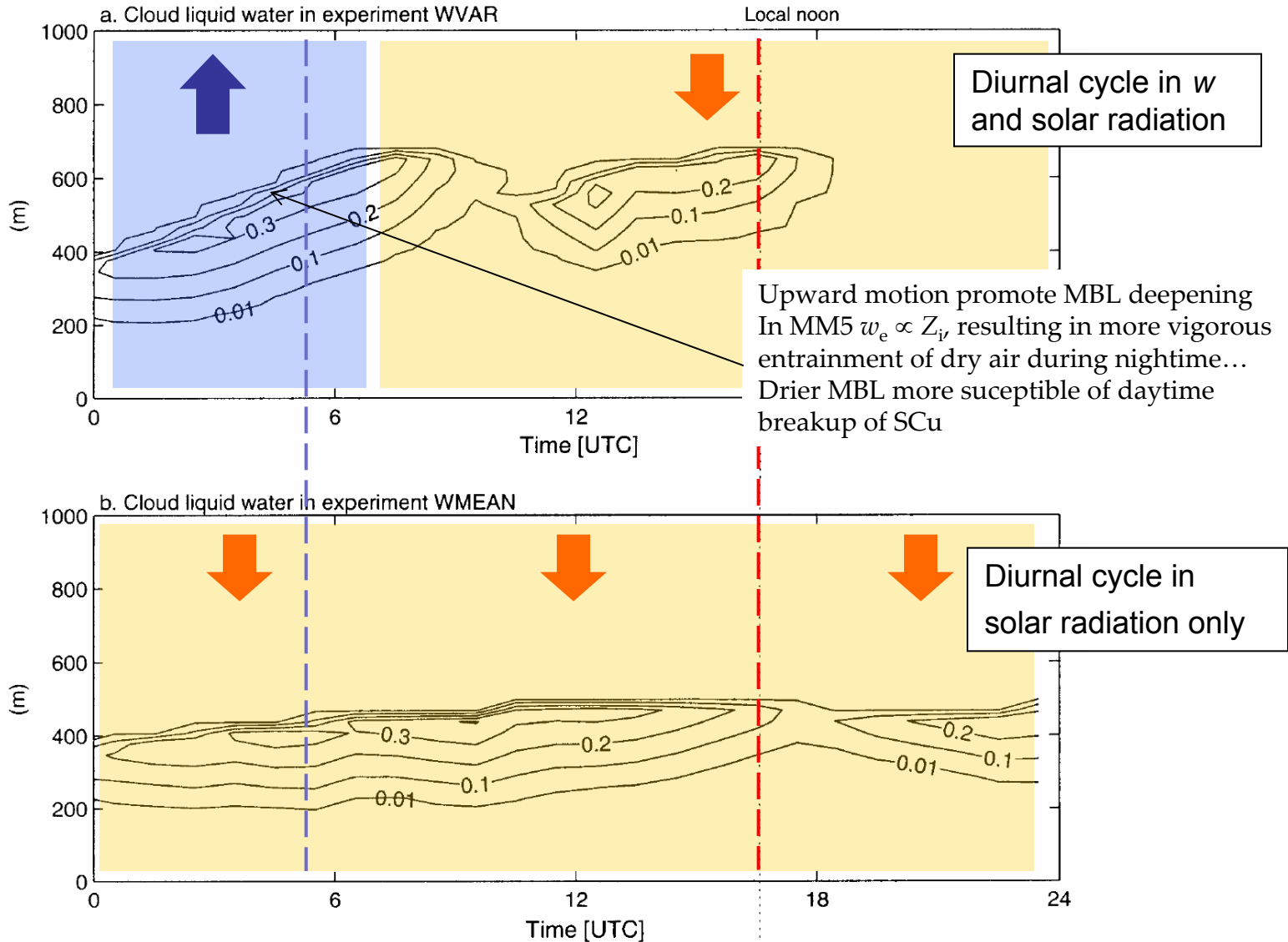
MM5 results. SON simulation.

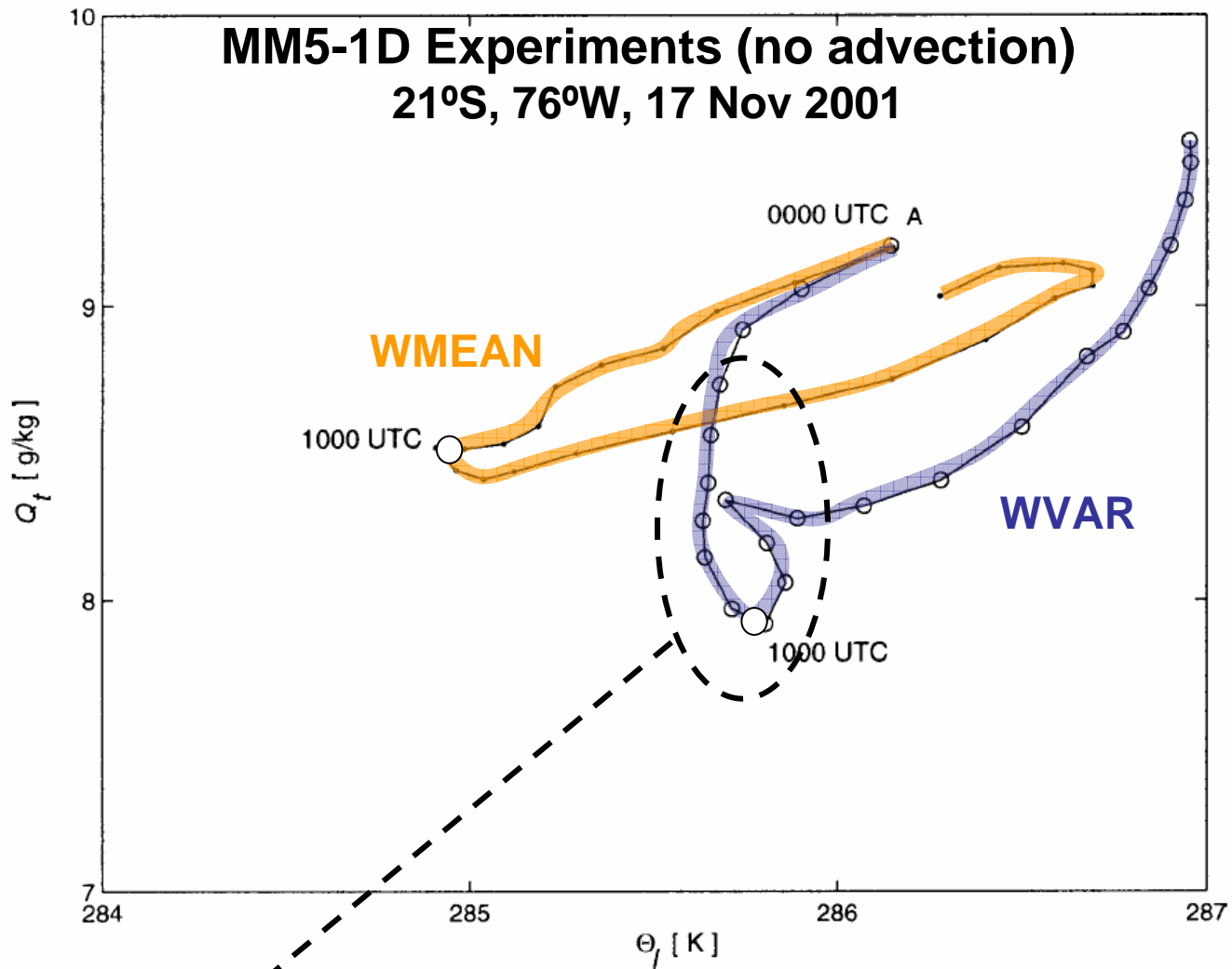


- Significant diurnal cycle in θ up to 5 km ASL
- Subsidence interrupted by period of upward motion
- Cooling largely produced by vertical advection

MM5-1D Experiments (no advection)

Impact dependent on location / interference with solar cycle
21°S, 76°W, 17 Nov 2001





Significant drying (and little cooling) during nighttime hours when upsidence prevails. Larger entrainment at the top of a deeper MBL. (W_{LS} influence the size of the eddies).

Modelling microphysical and meteorological controls on precipitation and cloud cellular structures in Southeast Pacific stratocumulus

H. Wang^{1,2,*}, G. Feingold², R. Wood³, and J. Kazil^{1,2}

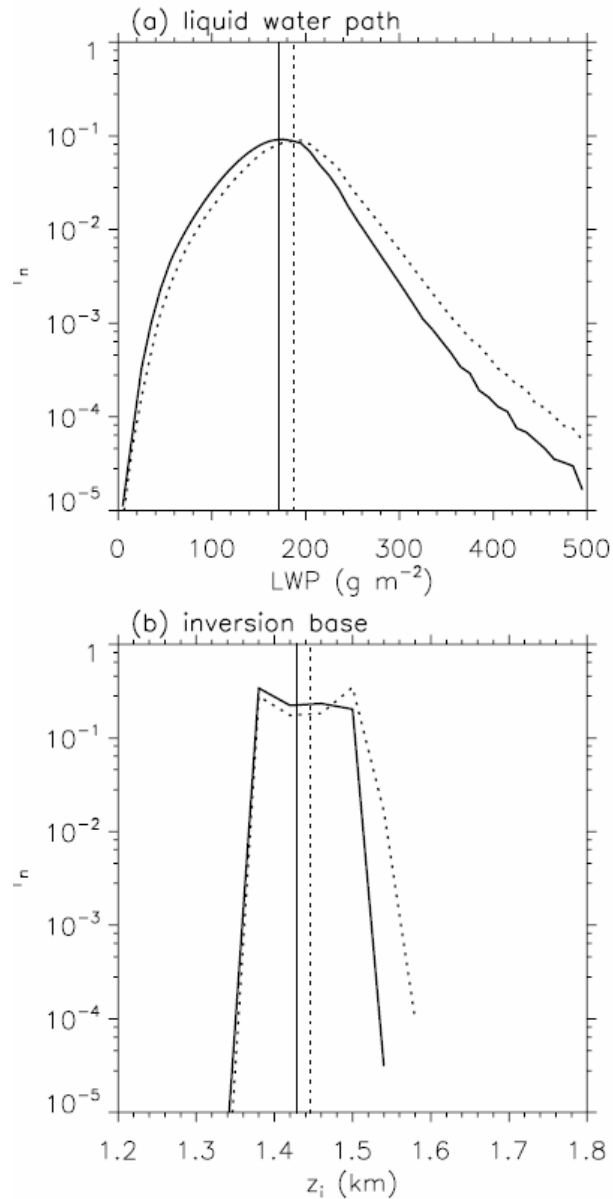


Fig. 9. Normalized frequency distributions of (a) liquid water path, (b) inversion base height over 8 h for experiments CTRL (solid lines) and UPSW (dotted lines) with the corresponding vertical lines indicating median values.

THE EPIC 2001 STRATOCUMULUS STUDY

BAMS 2004

BY CHRISTOPHER S. BREHERTON, TANEIL UTTAL, CHRISTOPHER W. FAIRALL, SANDRA E. YUTER,
ROBERT A. WELLER, DARREL BAUMGARDNER, KIMBERLY COMSTOCK, ROBERT WOOD, AND GRACIELA B. RAGA

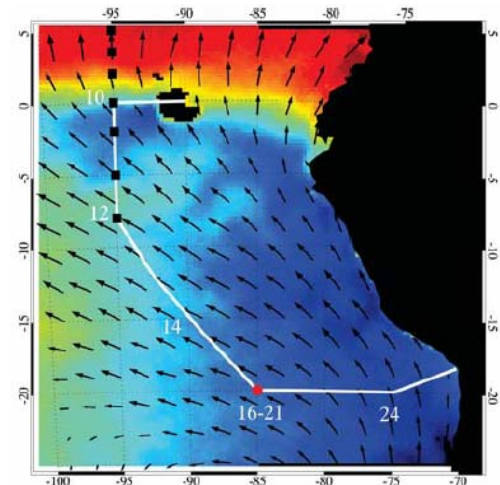
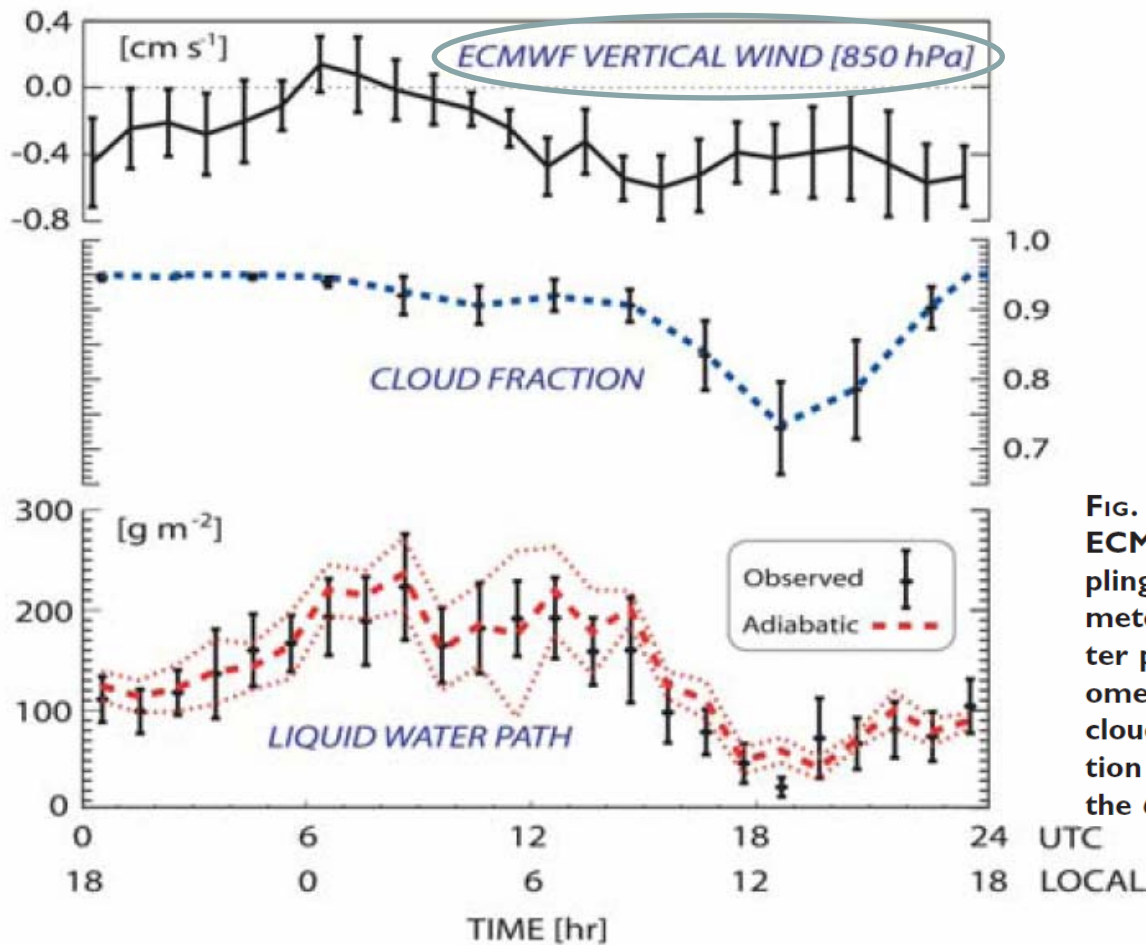
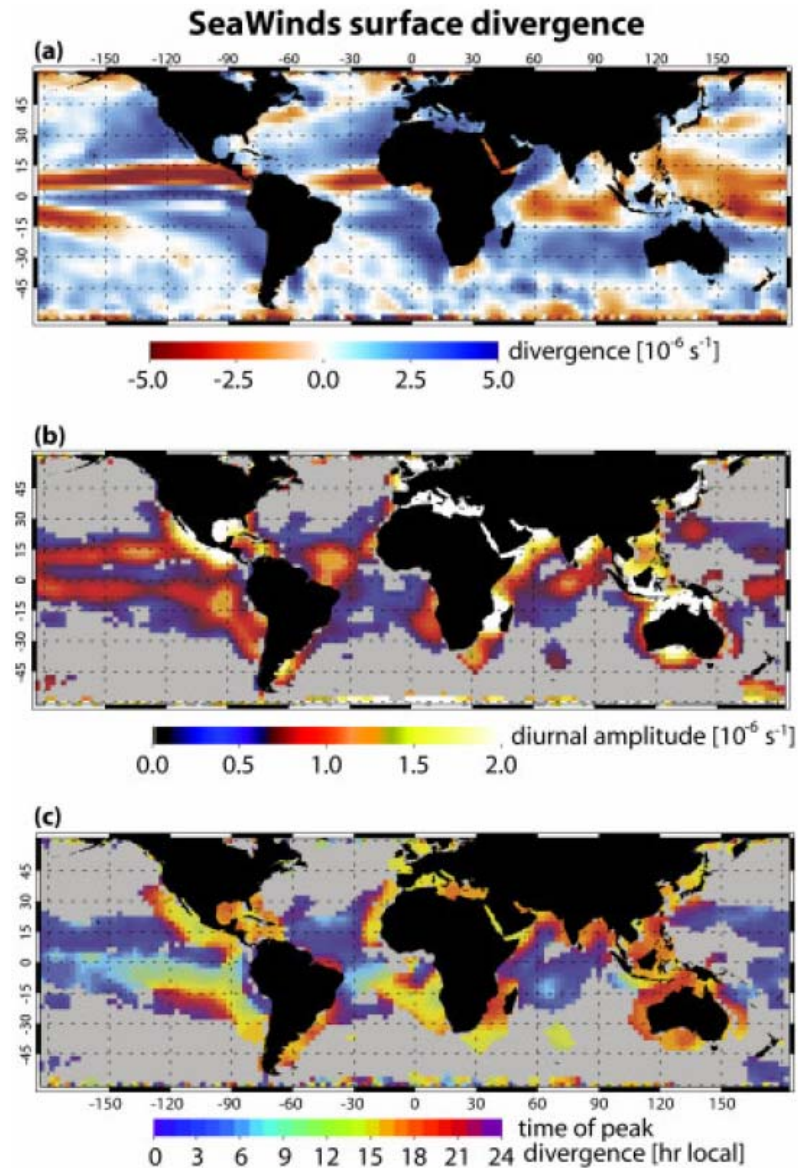


FIG. 6. The buoy-period mean diurnal cycle of (top) ECMWF-predicted vertical velocity from hourly sampling of 12–36-h operational forecasts, (middle) ceilometer-derived cloud fraction, and (bottom) liquid water path derived from the shipboard microwave radiometer, and adiabatic liquid water path derived from cloud thickness. Vertical bars show the standard deviation of hourly average values on individual days from the 6-day hourly mean.

The diurnal cycle of surface divergence over the global oceans

QJRMS 2009

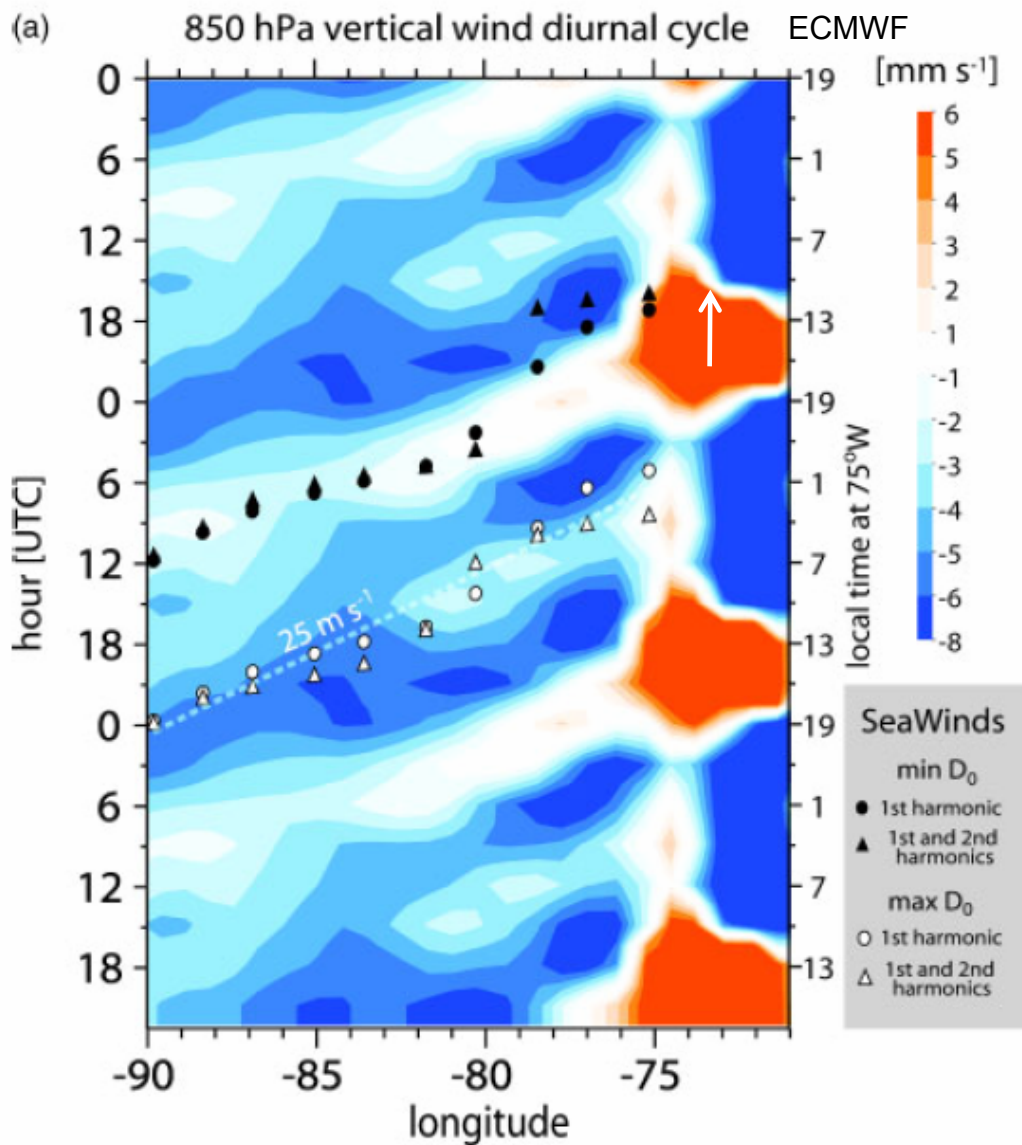
R. Wood,^{a*} M. Köhler,^b R. Bennartz^c and C. O'Dell^c



The diurnal cycle of surface divergence over the global oceans

QJRMS 2009

R. Wood,^{a*} M. Köhler,^b R. Bennartz^c and C. O'Dell^c



Marine boundary layer over the subtropical southeast Pacific during VOCALS-REx – Part 1: Mean structure and diurnal cycle

ACP 2010

D. A. Rahn and R. Garreaud

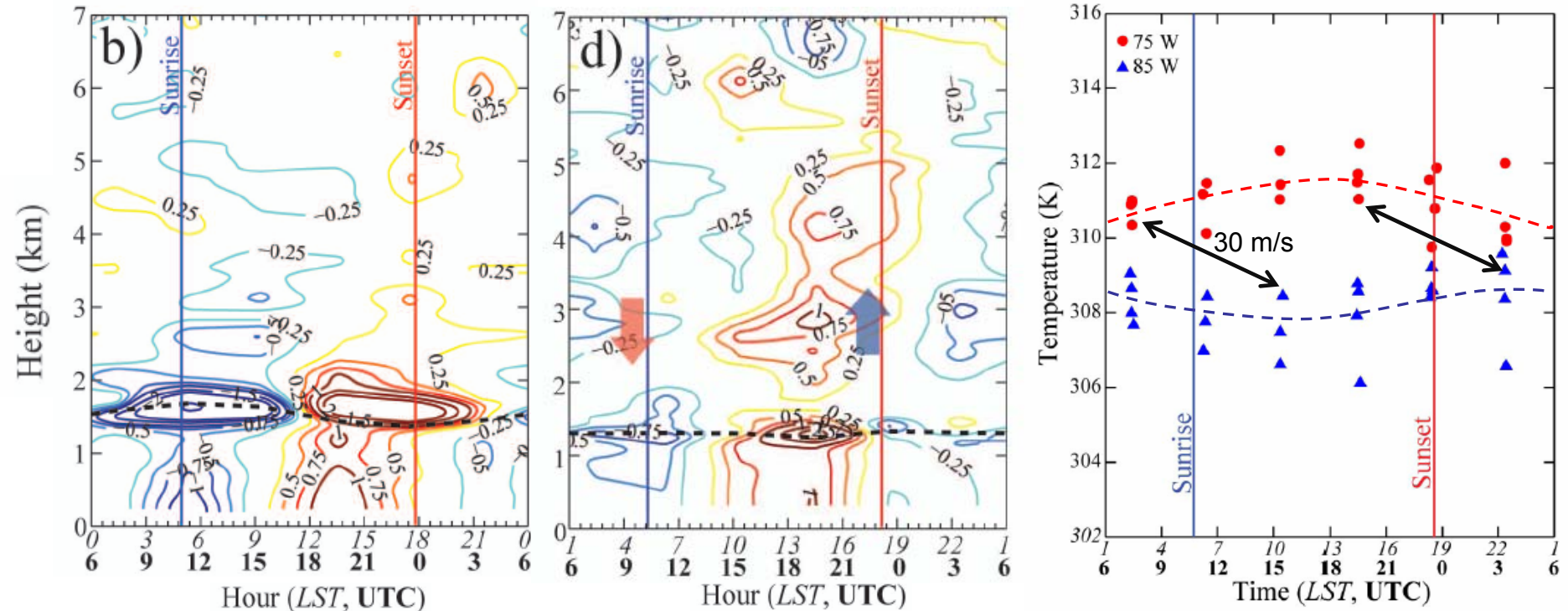
R/B Soundings during VOCALS-REx (add all Stratus Cruises!!!)

θ' hourly departure from 3-day mean

θ at 2.5 km

20°S 85°W

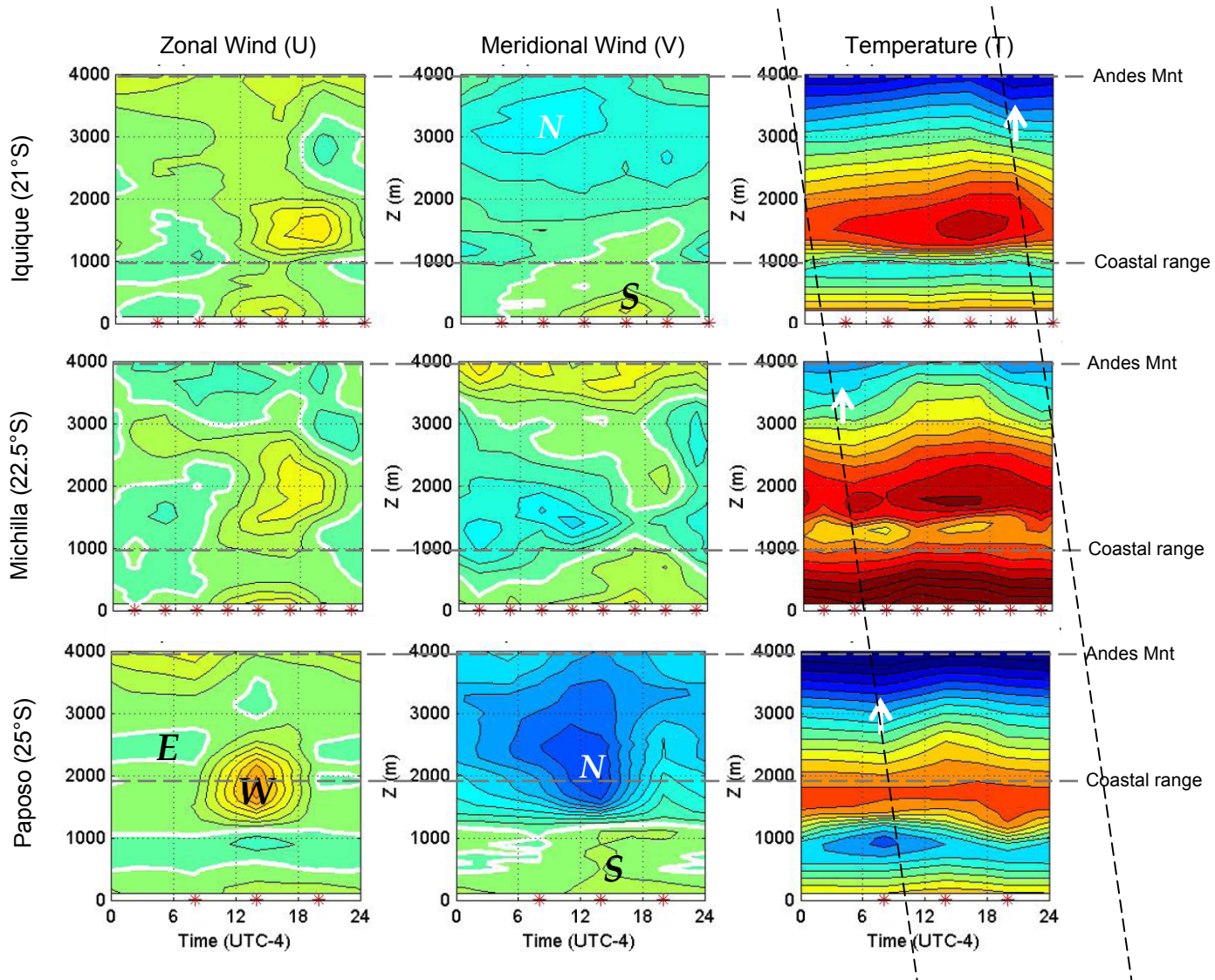
20°S 75°W



Observed coastal diurnal cycles

Paposo & Iquique: VOCAL-REx (Oct-Nov 2008)

Michilla: DICLIMA (January 1998)



Stratocumulus Cloud-Top Height Estimates and Their Climatic Implications

PAQUITA ZUIDEMA AND DAVID PAINEMAL
SIMON DE SZOEKE CHRIS FAIRALL

JClim 2009

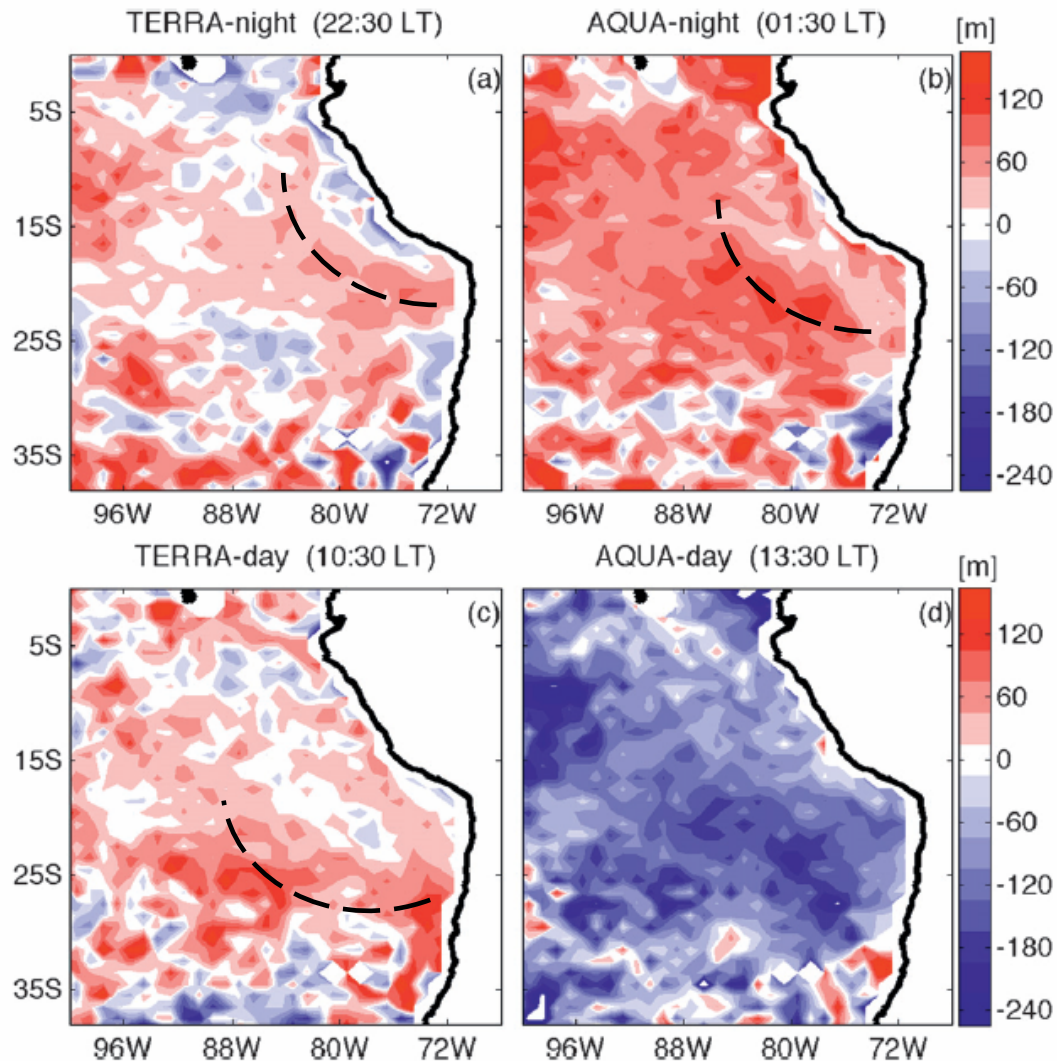
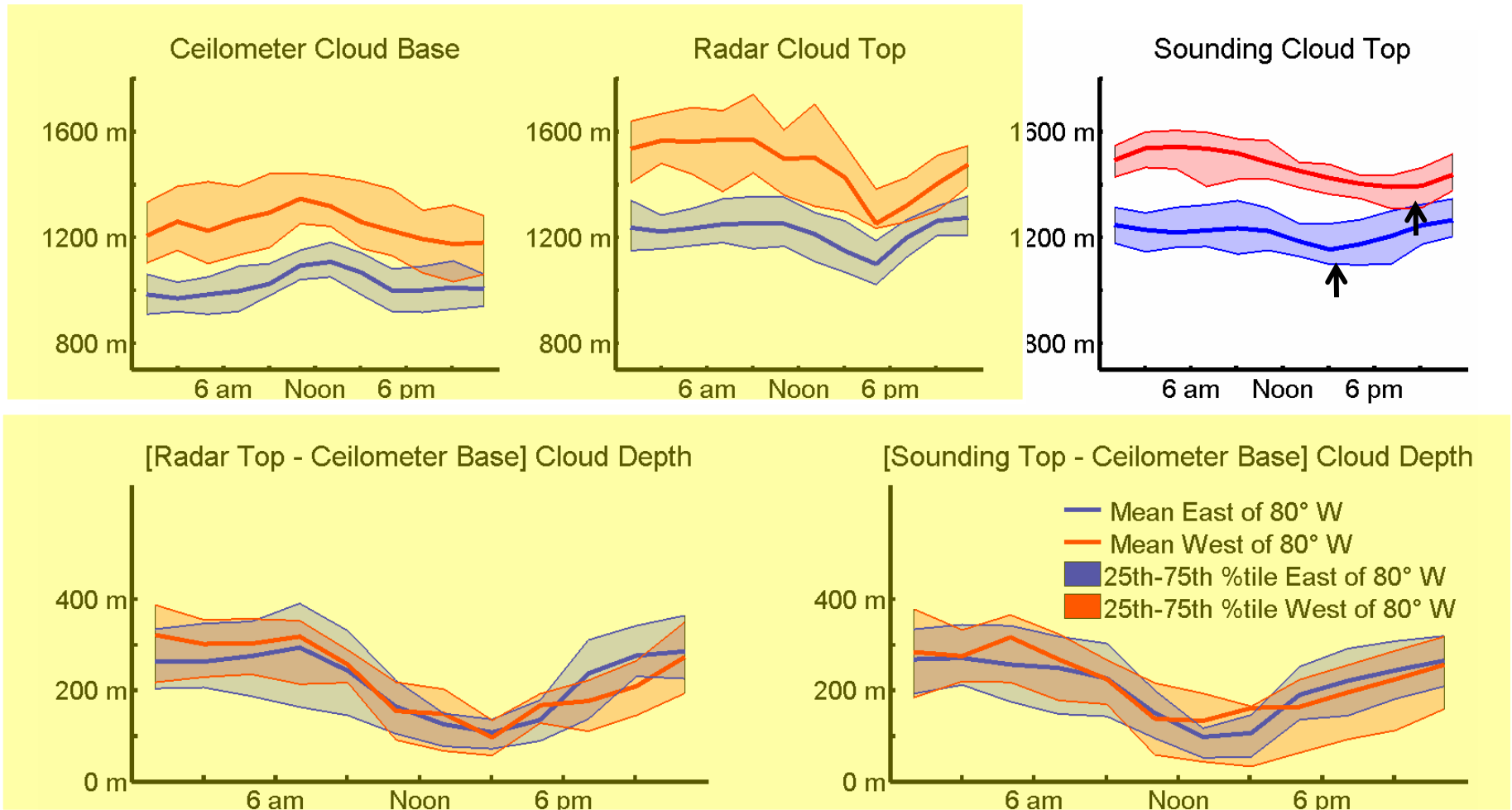


FIG. 10. Same as in Fig. 9, but here cloud-top heights are plotted as the anomaly from the 4-times-daily mean, and cloud fraction is not shown. The panels correspond to (a) *Terra* night, at 2230 LT, (b) *Aqua* night, at 0130 LT, (c) *Terra* day, at 1030 LT, and (d) *Aqua* day, at 1330 LT.

Observations of the Diurnal Cycle of Marine Stratocumulus Clouds and Precipitation

Casey Burleyson¹, Sandra Yuter¹, and Simon de Szoeke²



Mixed-Layer Budget Analysis of the Diurnal Cycle of Entrainment in Southeast Pacific Stratocumulus

JAS 2005

PETER CALDWELL, CHRISTOPHER S. BRETHERTON, AND ROBERT WOOD

w_e in observations shows a diurnal cycle similar to MM5 simulation, largely due to diurnal cycle in w_{LS}

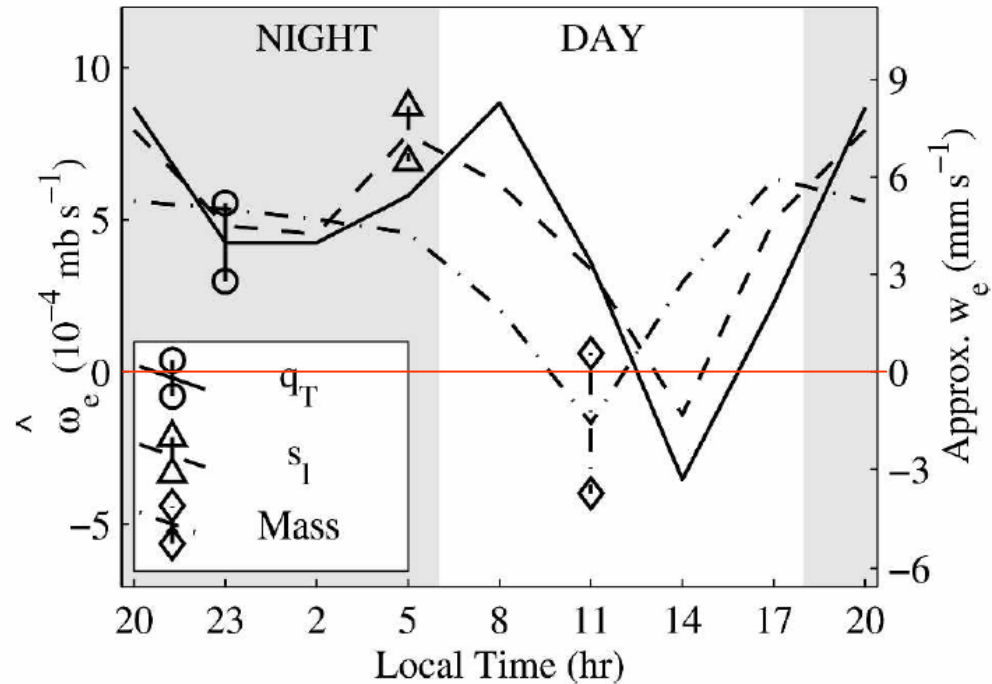


FIG. 7. Comparison of the diurnal cycle of entrainment as calculated from the q_t budget (solid lines, circular endpoints on error bar), from the s_t budget (dashed lines, triangular endpoint), and from the subsidence method (dot-dashed lines, diamond endpoint). Error bars represent one standard deviation limits on the mean associated with sample variability over the 6 days. Only one error bar is presented for each method because the error is assumed identical for each time of day.

Cloud Liquid Water Path from Satellite-Based Passive Microwave Observations: A New Climatology over the Global Oceans

JCim 2008

CHRISTOPHER W. O'DELL FRANK J. WENTZ RALF BENNARTZ

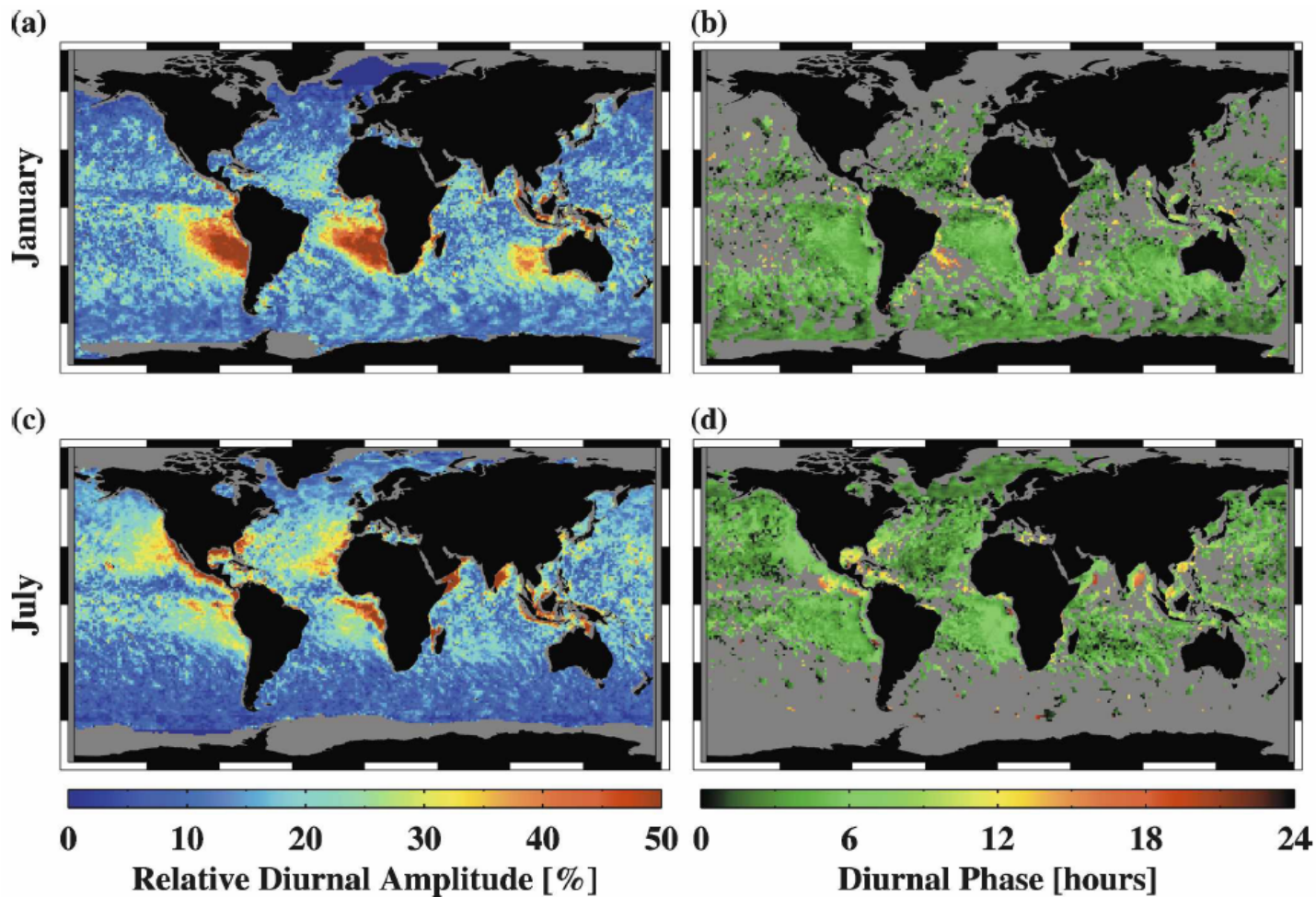


FIG. 10. Relative amplitude and phase of the diurnal cycle in the months of January and July. The diurnal cycle phase is the local time of maximum LWP. Black pixels denote land, while gray pixels denote missing data, from either the presence of sea ice or the close proximity of land; (b), (d) gray pixels also indicate locations without a well-defined diurnal maximum in LWP.

Cloud Liquid Water Path from Satellite-Based Passive Microwave Observations: A New Climatology over the Global Oceans

JCim 2008

CHRISTOPHER W. O'DELL FRANK J. WENTZ RALF BENNARTZ

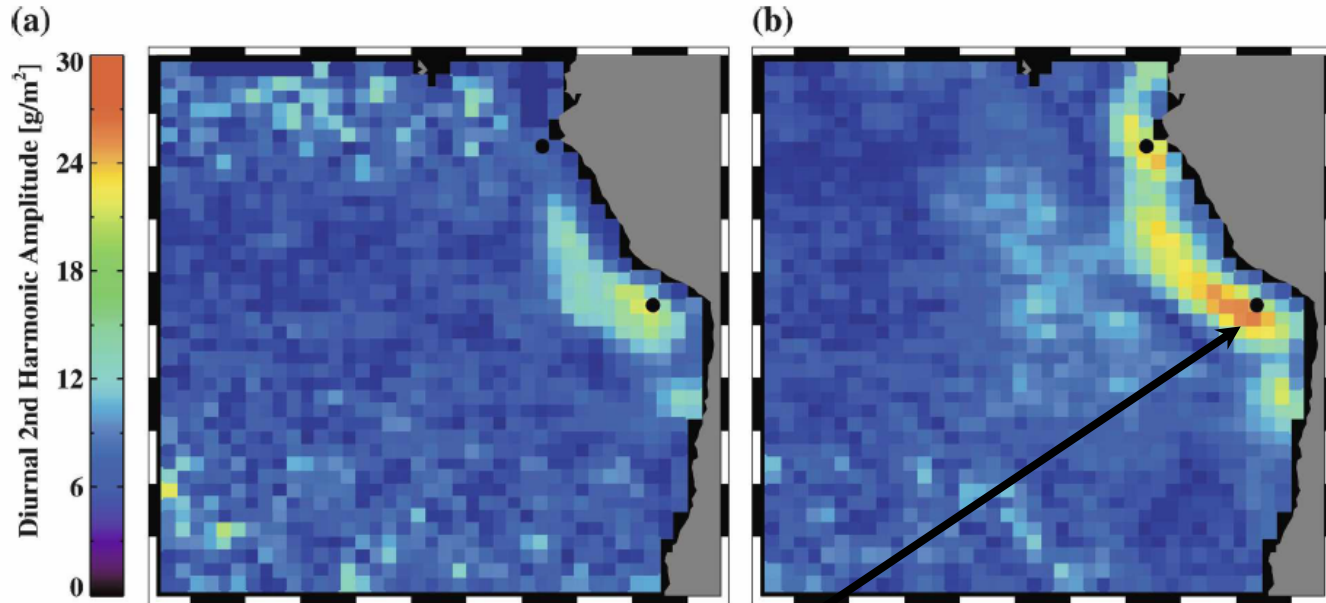
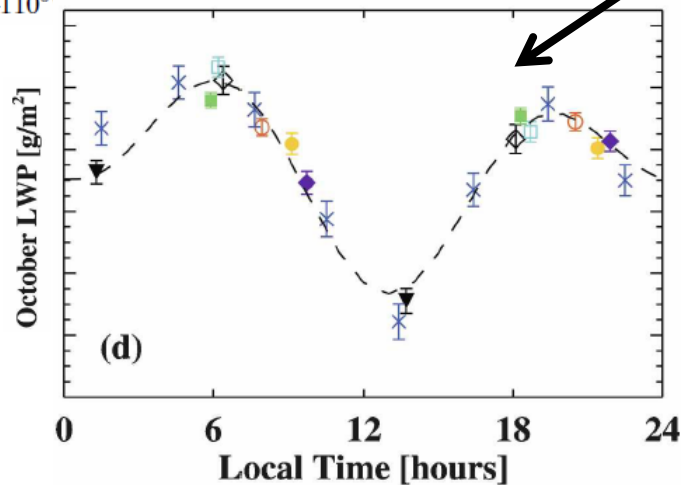


FIG. 11. Map of the amplitude of the second harmonic of the diurnal cycle for a region off the coast of South America for the months of April and October. The plotted region extends from the equator to 40°S, 70°–110°

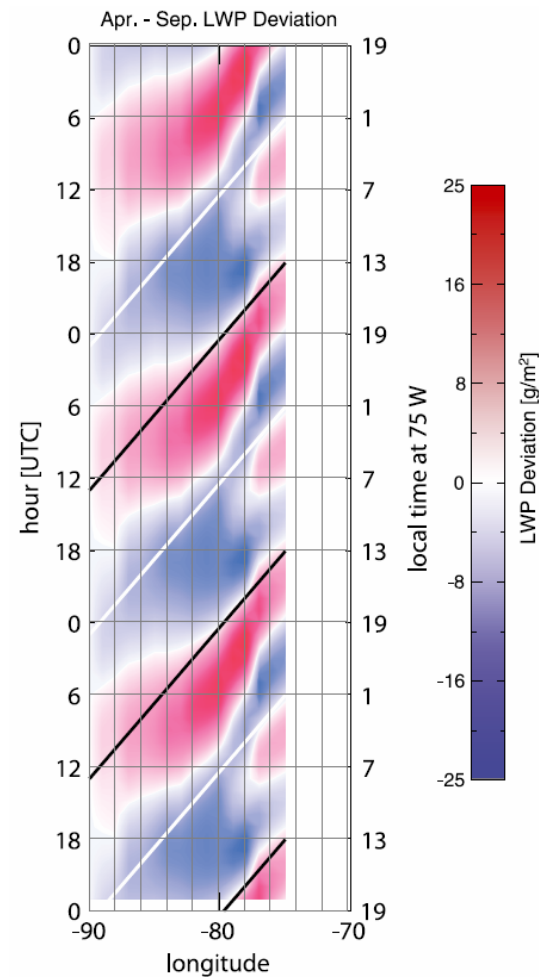
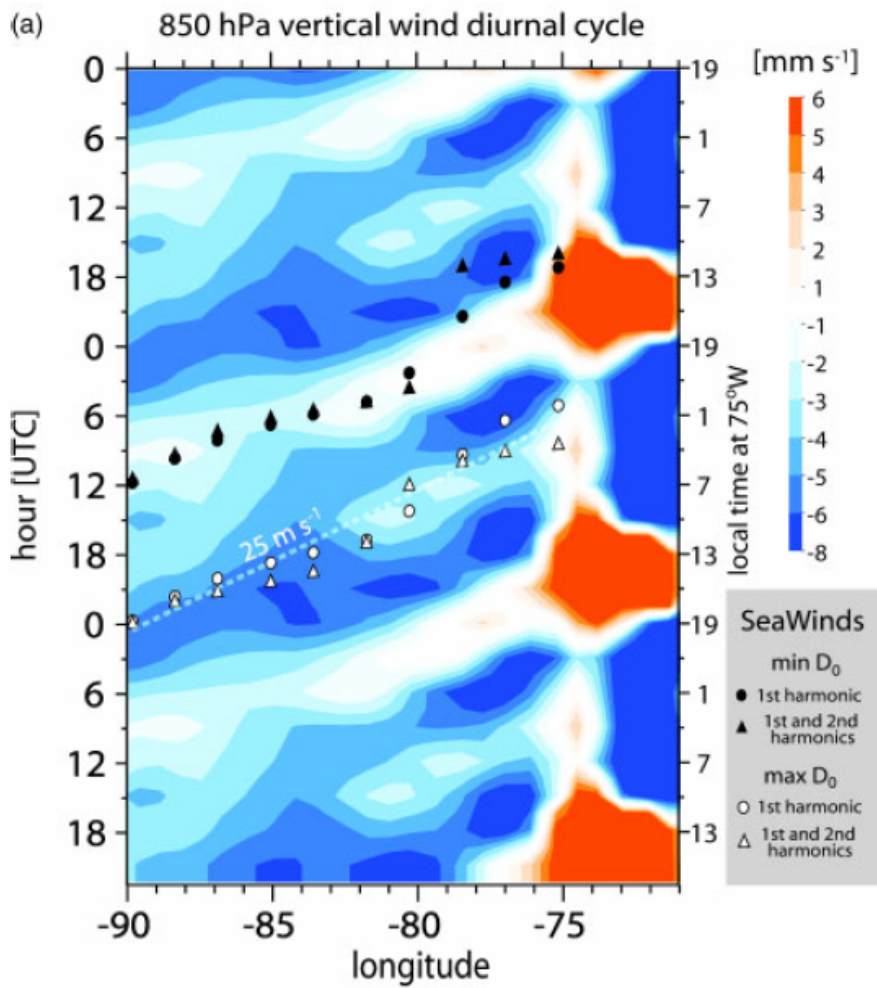


At this point, dominance of 12-h harmonic due to superposition of 24-h solar cycle and 24-h upsidence wave

The diurnal cycle of surface divergence over the global oceans

QJRMS 2009

R. Wood,^{a*} M. Köhler,^b R. Bennartz^c and C. O'Dell^c

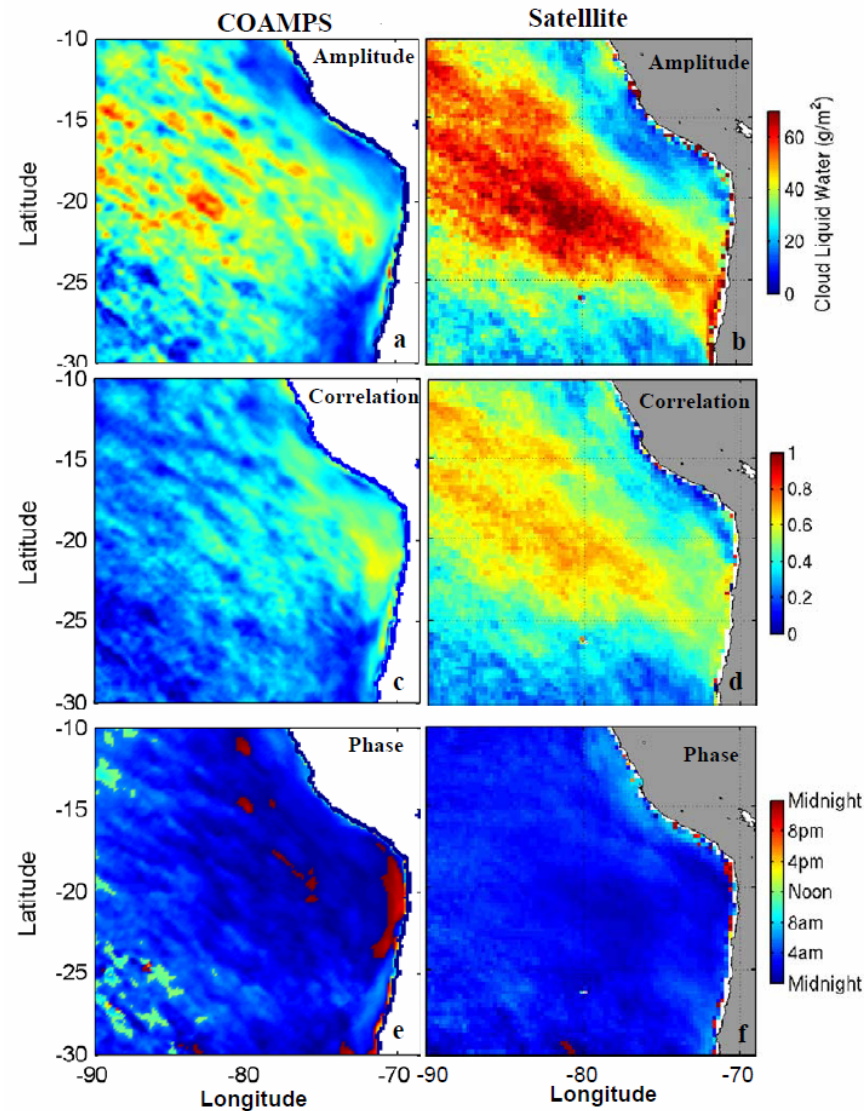


A regional real-time forecast of marine boundary layers during VOCALS-REx

ACP 2010

S. Wang¹, L. W. O'Neill², Q. Jiang¹, S. P. de Szoeke³, X. Hong¹, H. Jin¹, W. T. Thompson¹, and X. Zheng⁴

Fig. 4. Comparison of the harmonic analysis of LWP between the COAMPS forecasts (left column) and the satellite data (right column). (a) Predicted diurnal amplitude; (b) satellite diurnal amplitude; (c) correlation with the predicted harmonic diurnal function; (d) correlation with the satellite diurnal function; (e) local hours of the LWP maximum in the model; and (f) local hours of the LWP maximum in the satellite data.



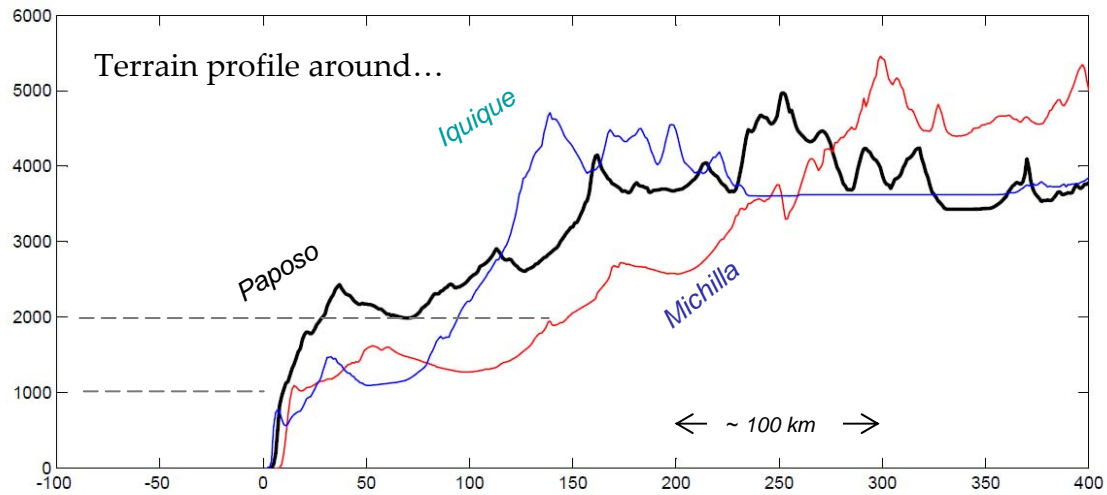
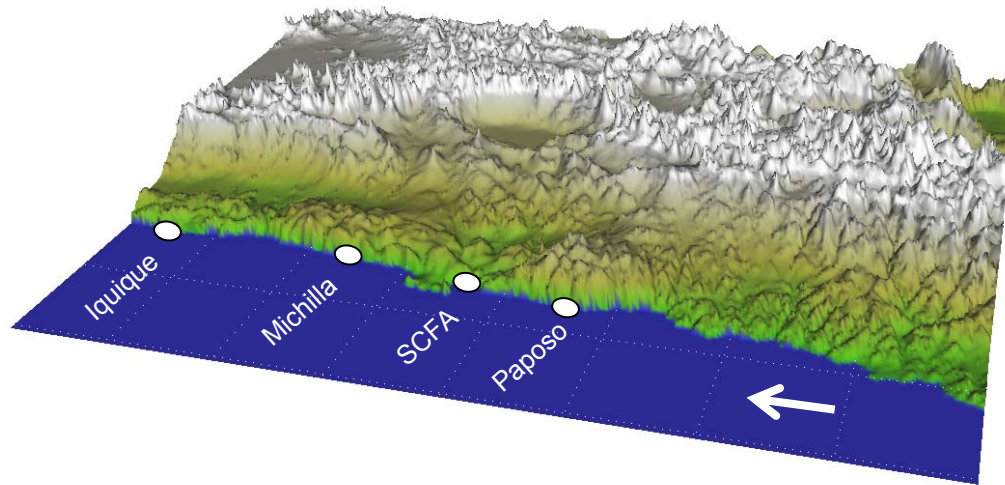
From pre-VOCALS and VOCALS-REx data, the *upsidence wave* (propagating offshore from the Southern Peruvian / Northern Chile coast) has an impact in the diurnal cycle of:

- | | |
|-------------------------------------|----------|
| * Mid-tropospheric θ and v | Yes |
| * Surface divergence | Yes |
| * Cloud top height | Could be |
| * Cloud fraction | Could be |
| * Cloud LWP | ??? |

Still pending origin of UpW....

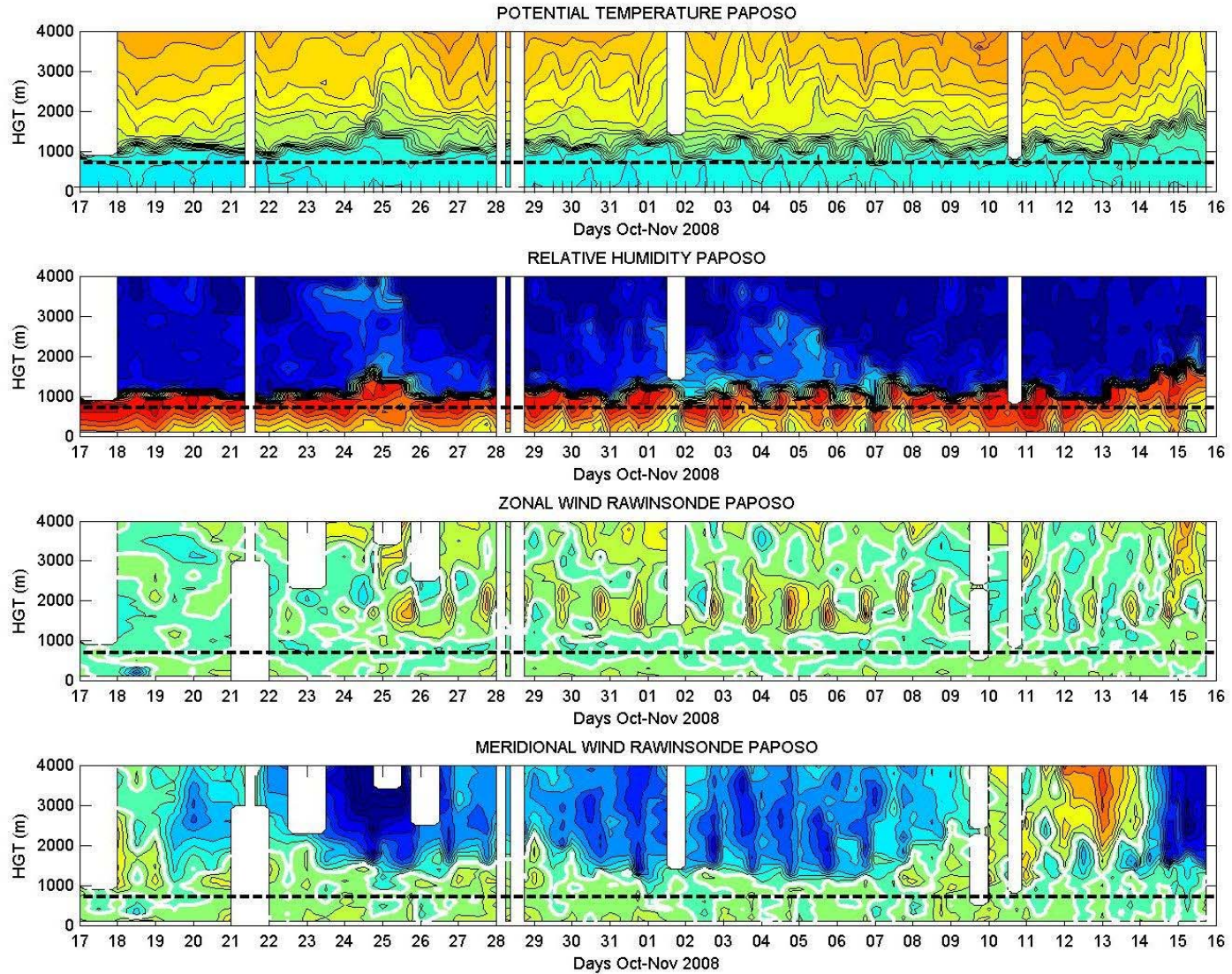
Coastal diurnal cycles

Relevant for airmass transport between continent and ocean



Coastal diurnal cycles

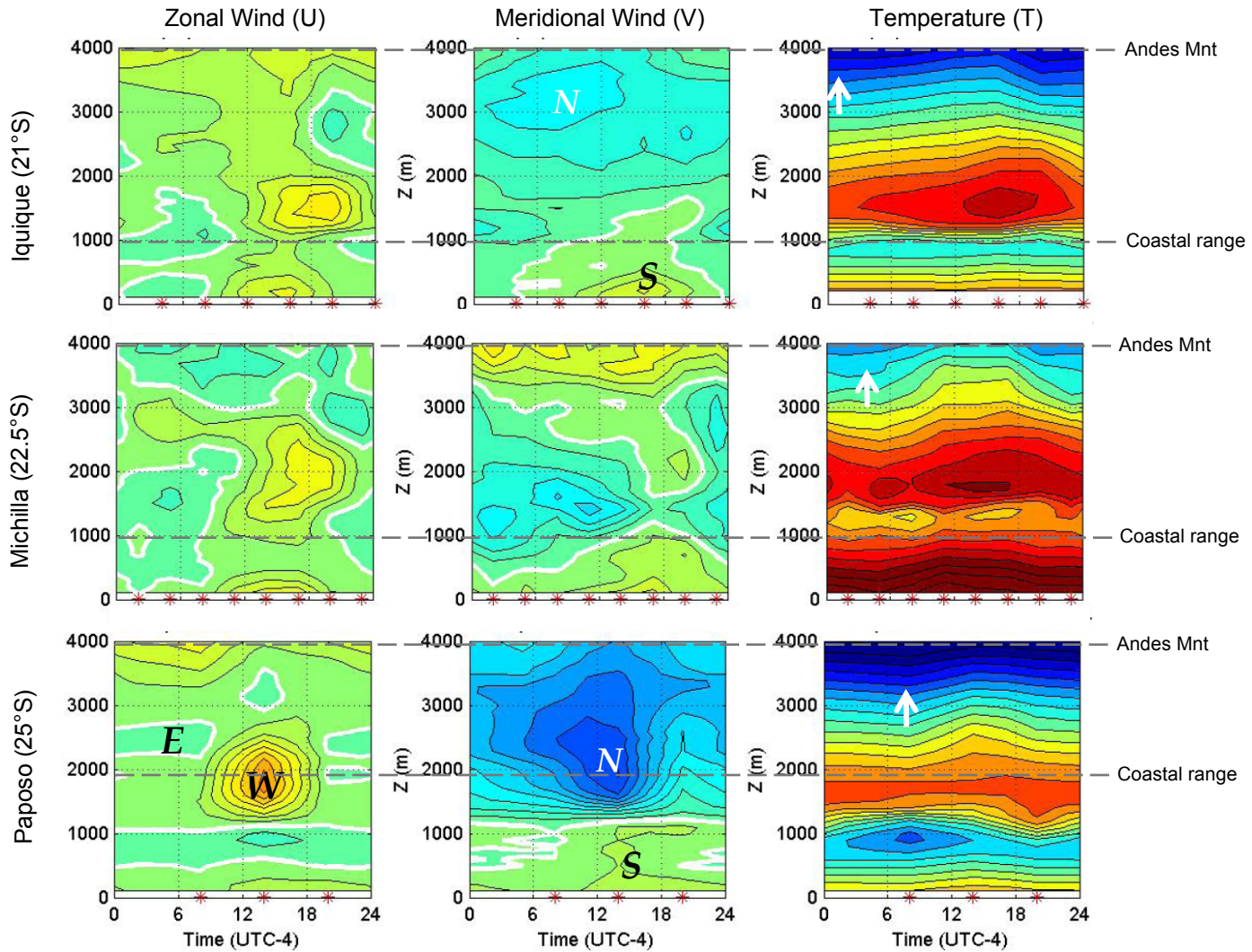
Relevant for air mass transport between continent and ocean



Observed coastal diurnal cycles

Paposo & Iquique: VOCAL-REx (Oct-Nov 2008)

Michilla: DICLIMA (January 1998)



Simulated diurnal cycle at Paposo (25°S)

WRF 15 km Simulation (Rhan and Garreaud 2010)

